

Shear band healing in amorphous materials by small-amplitude oscillatory shear deformation

Nikolai V. Priezjev^{1,2}

¹*Department of Mechanical and Materials Engineering,*

Wright State University, Dayton, OH 45435 and

²*National Research University Higher School of Economics, Moscow 101000, Russia*

(Dated: February 11, 2021)

Abstract

The effect of small-amplitude periodic shear on annealing of a shear band in binary glasses is investigated using molecular dynamics simulations. The shear band is first introduced in stable glasses via large-amplitude periodic shear, and then amorphous samples are subjected to repeated loading during thousands of cycles at strain amplitudes below the yield strain. It was found that with increasing strain amplitude, the glasses are relocated to deeper potential energy levels, while the energy change upon annealing is not affected by the glass initial stability. The results of mechanical tests indicate that the shear modulus and yield stress both increase towards plateau levels during the first few hundred cycles, and their magnitudes are largest when samples are loaded at strain amplitudes close to the yield strain. The analysis of nonaffine displacements reveals that the shear band breaks up into isolated clusters that gradually decay over time, leading to nearly reversible deformation within the elastic range. These results might be useful for mechanical processing of metallic glasses and additive manufacturing.

Keywords: metallic glasses, time periodic deformation, yielding transition, shear band, molecular dynamics simulations

I. INTRODUCTION

Understanding the structure evolution in amorphous alloys during thermal and mechanical treatments is important for tuning their physical and mechanical properties [1]. It is well accepted by now that in contrast to crystalline solids where plasticity is governed by topological line defects, known as disclinations, the elementary plastic events in amorphous materials involve collective rearrangements of a few tens of atoms or the so-called shear transformations [2, 3]. In a driven system, these rearrangements can assemble into shear bands where flow becomes sharply localized and act as a precursor for fracture [4–7]. Once a shear band is formed, the structural integrity can be recovered either by heating a sample above the glass transition temperature and then cooling back to the glass phase (resetting the structure) or, alternatively, via mechanical agitation. For example, it was shown using atomistic simulations that cracks in nanocrystalline metals can be completely healed via formation of wedge disclinations during stress-driven grain boundary migration [8]. It was also found experimentally and by means of atomistic simulations that after steady deformation of bulk metallic glasses, the shear bands relax during annealing below the glass transition temperature and the local diffusion coefficient exhibits a nonmonotonic behavior [9]. In the case of amorphous solids, however, the effects of periodic loading and initial glass stability on structural relaxation within the shear band domain, degree of annealing, and change in mechanical properties yet remain to be understood.

During the last decade, molecular dynamics simulations were particularly valuable in elucidating the atomic mechanisms of structural relaxation, rejuvenation, and yielding in amorphous materials under periodic loading conditions [10–39]. Remarkably, it was found that in athermal, disordered solids subjected to oscillatory shear in the elastic range, the trajectories of atoms after a number of transient cycles become exactly reversible and fall into the so-called ‘limit cycles’ [13, 15]. On the other hand, in the presence of thermal fluctuations, the relaxation process generally continues during thousands of cycles and the decay of the potential energy becomes progressively slower over time [22, 24, 29]. More recently, it was shown that the critical strain amplitude increases in more stable athermal glasses [35, 36], whereas the yielding transition can be significantly delayed in mechanically annealed binary glasses at finite temperature [39]. In general, the formation of a shear band during the yielding transition is accelerated in more rapidly annealed glasses periodically

loaded at a higher strain amplitude or when the shear orientation is alternated in two or three spatial dimensions [20, 23, 28, 31, 37]. Interestingly, after a shear band is formed during cyclic loading, the glass outside the band remains well annealed, and upon reducing strain amplitude below yield, the initial shear band anneals out, which leads to reversible dynamics in the whole domain [28]. However, despite extensive efforts, it remains unclear whether mechanical annealing of a shear band or a crack in metallic glasses depends on the preparation history, sample size and loading conditions.

In this paper, the influence of periodic shear deformation in the elastic range on shear band annealing and mechanical properties of binary glasses is studied using molecular dynamics simulations. The system-spanning shear band is initially formed in stable glasses that were either thermally or mechanically annealed. It will be shown that small-amplitude oscillatory shear anneals out the shear band and leads to nearly reversible deformation after a few hundred cycles at finite temperature. Moreover, upon loading at higher strain amplitudes, the glasses become increasingly better annealed, which results in higher yield stress.

The rest of the paper is outlined as follows. The preparation procedure, deformation protocol as well as the details of the simulation model are described in the next section. The time dependence of the potential energy, mechanical properties, and spatial organization of atoms with large nonaffine displacements are presented in section III. The results are briefly summarized in the last section.

II. MOLECULAR DYNAMICS (MD) SIMULATIONS

In the present study, the amorphous alloy is represented by the binary (80:20) Lennard-Jones (LJ) mixture originally introduced by Kob and Andersen (KA) about twenty years ago [40]. In this model, the interaction between different types of atoms is strongly non-additive, thus, allowing formation of a disordered structure upon slow cooling below the glass transition temperature [40]. More specifically, the pairwise interaction is modeled via the LJ potential, as follows:

$$V_{\alpha\beta}(r) = 4\varepsilon_{\alpha\beta} \left[\left(\frac{\sigma_{\alpha\beta}}{r} \right)^{12} - \left(\frac{\sigma_{\alpha\beta}}{r} \right)^6 \right], \quad (1)$$

with the parameters: $\varepsilon_{AA} = 1.0$, $\varepsilon_{AB} = 1.5$, $\varepsilon_{BB} = 0.5$, $\sigma_{AA} = 1.0$, $\sigma_{AB} = 0.8$, $\sigma_{BB} = 0.88$, and $m_A = m_B$ [40]. It should be mentioned that a similar parametrization was used by

Weber and Stillinger to study the amorphous metal-metalloid alloy Ni₈₀P₂₀ [41]. To save computational time, the LJ potential was truncated at the cutoff radius $r_{c,\alpha\beta} = 2.5 \sigma_{\alpha\beta}$. The total number of atoms is fixed $N = 60\,000$ throughout the study. For clarity, all physical quantities are reported in terms of the reduced units of length, mass, and energy $\sigma = \sigma_{AA}$, $m = m_A$, and $\varepsilon = \varepsilon_{AA}$. Using the LAMMPS parallel code, the equations of motion were integrated via the velocity Verlet algorithm with the time step $\Delta t_{MD} = 0.005 \tau$, where $\tau = \sigma \sqrt{m/\varepsilon}$ is the LJ time [42, 43].

All simulations were carried out at a constant density $\rho = \rho_A + \rho_B = 1.2 \sigma^{-3}$ in a periodic box of linear size $L = 36.84 \sigma$. It was previously found that the computer glass transition temperature of the KA model at the density $\rho = 1.2 \sigma^{-3}$ is $T_c = 0.435 \varepsilon/k_B$ [40]. The system temperature was maintained via the Nosé-Hoover thermostat [42, 43]. After thorough equilibration and gradual annealing at the temperature $T_{LJ} = 0.01 \varepsilon/k_B$, the system was subjected to periodic shear deformation along the xz plane as follows:

$$\gamma(t) = \gamma_0 \sin(2\pi t/T), \quad (2)$$

where γ_0 is the strain amplitude and $T = 5000 \tau$ is the period of oscillation. The corresponding oscillation frequency is $\omega = 2\pi/T = 1.26 \times 10^{-3} \tau^{-1}$. Once a shear band was formed at $\gamma_0 = 0.080$, the glasses were periodically strained at the strain amplitudes $\gamma_0 = 0.030, 0.040, 0.050, 0.060,$ and 0.065 during 3000 cycles. It was previously found that in the case of poorly annealed (rapidly cooled) glasses, the critical value of the strain amplitude at the temperature $T_{LJ} = 0.01 \varepsilon/k_B$ and density $\rho = 1.2 \sigma^{-3}$ is $\gamma_0 \approx 0.067$ [37]. The typical simulation during 3000 cycles takes about 80 days using 40 processors in parallel.

For the simulation results presented in the next section, the preparation and the initial loading protocols are the same as the ones used in the previous MD study on the yielding transition in stable glasses [39]. Briefly, the binary mixture was first equilibrated at $T_{LJ} = 1.0 \varepsilon/k_B$ and $\rho = 1.2 \sigma^{-3}$ and then slowly cooled with the rate $10^{-5} \varepsilon/k_B \tau$ to $T_{LJ} = 0.30 \varepsilon/k_B$. Furthermore, one sample was cooled down to $T_{LJ} = 0.01 \varepsilon/k_B$ during the time interval $10^4 \tau$ (see Fig. 1). The other sample was mechanically annealed at $T_{LJ} = 0.30 \varepsilon/k_B$ via cyclic loading at $\gamma_0 = 0.035$ during 600 cycles, and only then cooled to $T_{LJ} = 0.01 \varepsilon/k_B$ during $10^4 \tau$. Thus, after relocating glasses to $T_{LJ} = 0.01 \varepsilon/k_B$, two glass samples with different processing history and potential energies were obtained. In what follows, these samples will be referred to as *thermally annealed* and *mechanically annealed* glasses.

III. RESULTS

Amorphous alloys typically undergo physical aging, when a system slowly evolves towards lower energy states, and generally this process can be accelerated by external cyclic deformation within the elastic range [44]. Thus, the structural relaxation of disordered solids under periodic loading proceeds via collective, irreversible rearrangements of atoms [12, 22, 23, 25], while at sufficiently low energy levels, mechanical annealing becomes inefficient [35]. The two glass samples considered in the present study were prepared either via mechanical annealing at a temperature not far below the glass transition temperature or by computationally slow cooling from the liquid state. It was previously shown that small-amplitude periodic shear deformation at temperatures well below T_g does not lead to further annealing of these glasses [39]. Rather, the results presented below focus on the annealing process of a shear band, introduced in these samples by large periodic strain, and subsequent recovery of their mechanical properties.

The time dependence of the potential energy at the end of each cycle is reported in Fig. 2 for the *thermally annealed* glass. In this case, the glass was first subjected to oscillatory shear during 200 cycles with the strain amplitude $\gamma_0 = 0.080$ (see the black curve in Fig. 2). The strain amplitude $\gamma_0 = 0.080$ is slightly larger than the critical strain amplitude $\gamma_0 \approx 0.067$ at $T_{LJ} = 1.0 \varepsilon/k_B$ and $\rho = 1.2 \sigma^{-3}$ [37], and, therefore, the periodic loading induced the formation of a shear band across the system after about 20 cycles. As shown in Fig. 2, the process of shear band formation is associated with a sharp increase in the potential energy followed by a plateau at $U \approx -8.26 \varepsilon$ with pronounced fluctuations due to plastic flow within the band. It was previously demonstrated that during the plateau period, the periodic deformation involves two well separated domains with diffusive and reversible dynamics [39].

After the shear band became fully developed in the *thermally annealed* glass, the strain amplitude of periodic deformation was reduced in the range $0.030 \leq \gamma_0 \leq 0.065$ when $t = 200 T$. The results in Fig. 2 indicate that the potential energy of the system is gradually reduced when $t > 200 T$, and the energy drop increases at higher strain amplitudes (except for $\gamma_0 = 0.065$). Notice that the potential energy levels out at $t \gtrsim 1300 T$ for $\gamma_0 = 0.030$, 0.040 , and 0.050 , while the relaxation process continues up to $t = 3200 T$ for $\gamma_0 = 0.060$. These results imply that the shear band becomes effectively annealed by the small-amplitude

oscillatory shear, leading to nearly reversible dynamics in the whole sample, as will be illustrated below via the analysis of nonaffine displacements. By contrast, the deformation within the shear band remains irreversible at the higher strain amplitude $\gamma_0 = 0.065$ (denoted by the fluctuating grey curve in Fig. 2). This observation can be rationalized by realizing that the strain remains localized within the shear band, and the effective strain amplitude within the band is greater than the critical value $\gamma_0 \approx 0.067$ [37].

The potential energy minima for the *mechanically annealed* glass are presented in Fig. 3 for the indicated strain amplitudes. It should be commented that the preparation protocol, which included 600 cycles at $\gamma_0 = 0.035$ and $T_{LJ} = 0.30 \varepsilon/k_B$, produced an atomic configuration with a relatively deep potential energy level, *i.e.*, $U \approx -8.337 \varepsilon$. Upon periodic loading at $\gamma_0 = 0.080$ and $T_{LJ} = 0.01 \varepsilon/k_B$, the yielding transition is delayed by about 450 cycles, as shown by the black curve in Fig. 3 (the same data as in Ref. [39]). Similarly to the case of thermally annealed glasses, the potential energy in Fig. 3 is gradually reduced when the strain amplitude is changed from $\gamma_0 = 0.080$ to the selected values in the range $0.030 \leq \gamma_0 \leq 0.065$. Interestingly, the largest decrease in the potential energy at the strain amplitude $\gamma_0 = 0.060$ is nearly the same ($\Delta U \approx 0.03 \varepsilon$) for both thermally and mechanically annealed glasses. In addition, it can be commented that in both cases presented in Figs. 2 and 3, the potential energy remains above the energy levels of initially stable glasses (before a shear band is formed) even for loading at the strain amplitude $\gamma_0 = 0.060$. The results of a previous MD study on mechanical annealing of *rapidly quenched* glasses imply that the energy level $U \approx -8.31 \varepsilon$ can be reached via cyclic loading at $T_{LJ} = 0.01 \varepsilon/k_B$ but it might take thousands of additional cycles [37].

While the potential energy within a shear band becomes relatively large, the energy of the glass outside the band remains largely unaffected during the yielding transition. As shown above, the *mechanically annealed* glass is initially more stable (has a lower potential energy) than the *thermally annealed* glass. This in turn implies that the boundary conditions for the subyield loading of the shear band are different in the two cases, and, therefore, the potential energy change during the relaxation process, in principle, might also vary. In other words, the annealing of the shear band by small-amplitude periodic deformation might be affected by the atomic structure of the adjacent glass. However, the results in Figs. 2 and 3 suggest that the potential energy change is roughly the same in both cases; although a more careful

analysis might be needed in the future to clarify this point.

We next report the results of mechanical tests that involve startup continuous shear deformation in order to probe the effect of small-amplitude periodic loading on the yield stress. The shear modulus, G , and the peak value of the stress overshoot, σ_Y , are plotted in Figs. 4 and 5 for glasses that were periodically deformed with the strain amplitudes $\gamma_0 = 0.030$ and 0.060 . In each case, the startup deformation was imposed along the xy , xz , and yz planes with the constant strain rate $\dot{\gamma} = 10^{-5} \tau^{-1}$. The data are somewhat scattered, since simulations were carried out only for one realization of disorder, but the trends are evident. First, both G and σ_Y are relatively small when shear is applied along the xz plane at $t = 200 T$ in Fig. 4 and at $t = 1000 T$ in Fig. 5 because of the shear band that was formed previously at $\gamma_0 = 0.080$. Second, the shear modulus and yield stress increase towards plateau levels during the next few hundred cycles, and their magnitudes are greater for the larger strain amplitude $\gamma_0 = 0.060$, since those samples were annealed to deeper energy states (see Figs. 2 and 3).

The results in Figures 4 (b) and 5 (b) show that the yield stress is only weakly dependent on the number of cycles in glasses that were periodically strained at the smaller amplitude $\gamma_0 = 0.030$, whereas for $\gamma_0 = 0.060$, the yield stress increases noticeably and levels out at $\sigma_Y \approx 0.9 \varepsilon \sigma^{-3}$ for the *mechanically annealed* glass and at a slightly smaller value for the *thermally annealed* glass. It was previously shown that the yield stress is slightly larger, *i.e.*, $\sigma_Y \approx 1.05 \varepsilon \sigma^{-3}$, for rapidly quenched glasses that were mechanically annealed at the strain amplitude $\gamma_0 = 0.060$ for similar loading conditions [29]. This discrepancy might arise because in Ref. [29] the glass was homogeneously annealed starting from the rapidly quenched state, while in the present study, the potential energy within the annealed shear-band domain always remains higher than in the rest of the sample, thus resulting in spatially heterogeneous structure. On the other hand, it was recently shown that the presence of an interface between relaxed and rejuvenated domains in a relatively large sample might impede strain localization [45].

The relative rearrangements of atoms with respect to their neighbors in a deformed amorphous system can be conveniently quantified via the so-called nonaffine displacements. By definition, the nonaffine measure $D^2(t, \Delta t)$ for an atom i is computed via the transformation

matrix \mathbf{J}_i that minimizes the following expression for a group of neighboring atoms:

$$D^2(t, \Delta t) = \frac{1}{N_i} \sum_{j=1}^{N_i} \left\{ \mathbf{r}_j(t + \Delta t) - \mathbf{r}_i(t + \Delta t) - \mathbf{J}_i [\mathbf{r}_j(t) - \mathbf{r}_i(t)] \right\}^2, \quad (3)$$

where Δt is the time interval between two atomic configurations, and the summation is performed over the nearest neighbors located within 1.5σ from the position of the i -th atom at $\mathbf{r}_i(t)$. The nonaffine quantity defined by Eq. (3) was originally introduced by Falk and Langer in order to accurately detect the localized shear transformations that involved swift rearrangements of small groups of atoms in driven disordered solids [46]. In the last few years, this method was widely used to study the collective, irreversible dynamics of atoms in binary glasses subjected to time periodic [16, 18, 20, 22, 23, 29, 31, 32, 35, 37] and startup continuous [47–53] shear deformation, tension-compression cyclic loading [24, 33], prolonged elastostatic compression [54, 55], creep [56] and thermal cyclic loading [57–61].

The representative snapshots of *thermally annealed* glasses are presented in Fig. 6 for the strain amplitude $\gamma_0 = 0.030$ and in Fig. 7 for $\gamma_0 = 0.060$. For clarity, only atoms with relatively large nonaffine displacements during one oscillation period are displayed. Note that the typical cage size at $\rho = 1.2\sigma^{-3}$ is about 0.1σ [11], and, therefore, the displacements of atoms with $D^2(nT, T) > 0.04\sigma^2$ correspond to cage-breaking events. It can be clearly seen in the panel (a) of Figures 6 and 7, that the shear band runs along the yz plane right after switching to the subyield loading regime. As expected, the magnitude of $D^2(200T, T)$ on average decays towards the interfaces. Upon continued loading, the shear band becomes thinner and eventually breaks up into isolated clusters whose size is reduced over time. The coarsening process is significantly slower for the strain amplitude $\gamma_0 = 0.060$ (about 1000 cycles) than for $\gamma_0 = 0.030$ (about 200 cycles). This trend is consistent with the decay of the potential energy denoted in Fig. 2 by the red and orange curves.

Similar conclusions can be drawn by visual inspection of consecutive snapshots of the *mechanically annealed* glass cyclically loaded at the strain amplitude $\gamma_0 = 0.030$ (see Fig. 8) and at $\gamma_0 = 0.060$ (see Fig. 9). It can be observed that the shear band is initially oriented along the xy plane, which is consistent with a relatively large value of the yield stress along the xy direction at $t = 1000T$ in Fig. 5. The atomic trajectories become nearly reversible already after about 10 cycles at the strain amplitude $\gamma_0 = 0.030$, as shown in Fig. 8, while isolated clusters of atoms with large nonaffine displacements are still present after about

2000 cycles at $\gamma_0 = 0.060$ (see Fig. 9). Altogether these results indicate that oscillatory shear deformation with a strain amplitude just below the critical value can be used to effectively anneal a shear band and make the amorphous material stronger.

IV. CONCLUSIONS

In summary, the process of shear band annealing in metallic glasses subjected to small-amplitude periodic shear deformation was examined using molecular dynamics simulations. The glass was modeled as a binary mixture with non-additive interaction between atoms of different types, and the shear band was initially developed in stable glasses under oscillatory shear above the yielding point. It was shown that periodic loading in the elastic range results in a gradual decay of the potential energy over consecutive cycles, and upon increasing strain amplitude, lower energy states can be accessed after thousands of cycles. Furthermore, the spatiotemporal analysis of nonaffine displacements demonstrated that a shear band becomes thinner and breaks into separate clusters whose size is reduced upon continued loading. Thus, in a wide range of strain amplitudes below yield, the cyclic loading leads to a nearly reversible dynamics of atoms at finite temperature. Lastly, both the shear modulus and yield stress saturate to higher values as the shear band region becomes better annealed at higher strain amplitudes.

Acknowledgments

Financial support from the National Science Foundation (CNS-1531923) is gratefully acknowledged. The article was prepared within the framework of the HSE University Basic Research Program and funded in part by the Russian Academic Excellence Project ‘5-100’. The simulations were performed at Wright State University’s Computing Facility and the Ohio Supercomputer Center. The molecular dynamics simulations were carried out using the parallel LAMMPS code developed at Sandia National Laboratories [42].

-
- [1] Y. Sun, A. Concustell, and A. L. Greer, Thermomechanical processing of metallic glasses: Extending the range of the glassy state, *Nat. Rev. Mater.* **1**, 16039 (2016).

- [2] F. Spaepen, A microscopic mechanism for steady state inhomogeneous flow in metallic glasses, *Acta Metall.* **25**, 407 (1977).
- [3] A. S. Argon, Plastic deformation in metallic glasses, *Acta Metall.* **27**, 47 (1979).
- [4] B. A. Sun and W. H. Wang, The fracture of bulk metallic glasses, *Prog. Mater. Sci.* **74**, 211 (2015).
- [5] C. Zhong, H. Zhang, Q. P. Cao, X. D. Wang, D. X. Zhang, U. Ramamurty, and J. Z. Jiang, Size distribution of shear transformation zones and their evolution towards the formation of shear bands in metallic glasses, *J. Non-Cryst. Solids* **445**, 61 (2016).
- [6] V. Hieronymus-Schmidt, H. Rosner, G. Wilde, and A. Zaccone, Shear banding in metallic glasses described by alignments of Eshelby quadrupoles, *Phys. Rev. B* **95**, 134111 (2017).
- [7] D. Söpu, A. Stukowski, M. Stoica, and S. Scudino, Atomic-level processes of shear band nucleation in metallic glasses, *Phys. Rev. Lett.* **119**, 195503 (2017).
- [8] G. Q. Xu and M. J. Demkowicz, Healing of nanocracks by disclinations, *Phys. Rev. Lett.* **111**, 145501 (2013).
- [9] I. Binkowski, G. P. Shrivastav, J. Horbach, S. V. Divinski, and G. Wilde, Shear band relaxation in a deformed bulk metallic glass, *Acta Materialia* **109**, 330 (2016).
- [10] D. J. Lacks and M. J. Osborne, Energy landscape picture of overaging and rejuvenation in a sheared glass, *Phys. Rev. Lett.* **93**, 255501 (2004).
- [11] N. V. Priezjev, Heterogeneous relaxation dynamics in amorphous materials under cyclic loading, *Phys. Rev. E* **87**, 052302 (2013).
- [12] D. Fiocco, G. Foffi, and S. Sastry, Oscillatory athermal quasistatic deformation of a model glass, *Phys. Rev. E* **88**, 020301(R) (2013).
- [13] I. Regev, T. Lookman, and C. Reichhardt, Onset of irreversibility and chaos in amorphous solids under periodic shear, *Phys. Rev. E* **88**, 062401 (2013).
- [14] N. V. Priezjev, Dynamical heterogeneity in periodically deformed polymer glasses, *Phys. Rev. E* **89**, 012601 (2014).
- [15] I. Regev, J. Weber, C. Reichhardt, K. A. Dahmen, and T. Lookman, Reversibility and criticality in amorphous solids, *Nat. Commun.* **6**, 8805 (2015).
- [16] N. V. Priezjev, Reversible plastic events during oscillatory deformation of amorphous solids, *Phys. Rev. E* **93**, 013001 (2016).
- [17] T. Kawasaki and L. Berthier, Macroscopic yielding in jammed solids is accompanied by a

- non-equilibrium first-order transition in particle trajectories, *Phys. Rev. E* **94**, 022615 (2016).
- [18] N. V. Priezjev, Nonaffine rearrangements of atoms in deformed and quiescent binary glasses, *Phys. Rev. E* **94**, 023004 (2016).
- [19] P. Leishangthem, A. D. S. Parmar, and S. Sastry, The yielding transition in amorphous solids under oscillatory shear deformation, *Nat. Commun.* **8**, 14653 (2017).
- [20] N. V. Priezjev, Collective nonaffine displacements in amorphous materials during large-amplitude oscillatory shear, *Phys. Rev. E* **95**, 023002 (2017).
- [21] M. Fan, M. Wang, K. Zhang, Y. Liu, J. Schroers, M. D. Shattuck, and C. S. O'Hern, The effects of cooling rate on particle rearrangement statistics: Rapidly cooled glasses are more ductile and less reversible, *Phys. Rev. E* **95**, 022611 (2017).
- [22] N. V. Priezjev, Molecular dynamics simulations of the mechanical annealing process in metallic glasses: Effects of strain amplitude and temperature, *J. Non-Cryst. Solids* **479**, 42 (2018).
- [23] N. V. Priezjev, The yielding transition in periodically sheared binary glasses at finite temperature, *Comput. Mater. Sci.* **150**, 162 (2018).
- [24] N. V. Priezjev, Slow relaxation dynamics in binary glasses during stress-controlled, tension-compression cyclic loading, *Comput. Mater. Sci.* **153**, 235 (2018).
- [25] P. Das, A. D. S. Parmar, and S. Sastry, Annealing glasses by cyclic shear deformation (2018). arXiv:1805.12476
- [26] N. V. Priezjev and M. A. Makeev, The influence of periodic shear on structural relaxation and pore redistribution in binary glasses, *J. Non-Cryst. Solids* **506**, 14 (2019).
- [27] N. V. Priezjev and M. A. Makeev, Structural transformations during periodic deformation of low-porosity amorphous materials, *Modelling Simul. Mater. Sci. Eng.* **27**, 025004 (2019).
- [28] A. D. S. Parmar, S. Kumar, and S. Sastry, Strain localization above the yielding point in cyclically deformed glasses, *Phys. Rev. X* **9**, 021018 (2019).
- [29] N. V. Priezjev, Accelerated relaxation in disordered solids under cyclic loading with alternating shear orientation, *J. Non-Cryst. Solids* **525**, 119683 (2019).
- [30] E. Schinasi-Lemberg and I. Regev, Annealing and rejuvenation in a two-dimensional model amorphous solid under oscillatory shear, *Phys. Rev. E* **101**, 012603 (2020).
- [31] N. V. Priezjev, Shear band formation in amorphous materials under oscillatory shear deformation, *Metals* **10**, 300 (2020).
- [32] H. Li, H. Liu, and H. Peng, Atomic dynamics under oscillatory shear in metallic glasses, *J.*

- Non-Cryst. Solids **539**, 120069 (2020).
- [33] P. K. Jana and N. V. Priezjev, Structural relaxation in amorphous materials under cyclic tension-compression loading, *J. Non-Cryst. Solids* **540**, 120098 (2020).
- [34] T. Kawasaki and A. Onuki, Acoustic resonance in periodically sheared glass: damping due to plastic events, *Soft Matter* **16**, 9357 (2020).
- [35] W.-T. Yeh, M. Ozawa, K. Miyazaki, T. Kawasaki, and L. Berthier, Glass stability changes the nature of yielding under oscillatory shear, *Phys. Rev. Lett.* **124**, 225502 (2020).
- [36] H. Bhaumik, G. Foffi, and S. Sastry, The role of annealing in determining the yielding behavior of glasses under cyclic shear deformation (2020). arXiv:1911.12957
- [37] N. V. Priezjev, Alternating shear orientation during cyclic loading facilitates yielding in amorphous materials, *J. Mater. Eng. Perform.* **29**, 7328 (2020).
- [38] G.-J. Lyu, J.-C. Qiao, Y. Yao, J.-M. Pelletier, D. Rodney, J. Morthomas, and C. Fusco, Dynamic correspondence principle in the viscoelasticity of metallic glasses, *Scripta Materialia* **174**, 39 (2020).
- [39] N. V. Priezjev, A delayed yielding transition in mechanically annealed binary glasses at finite temperature, *J. Non-Cryst. Solids* **548**, 120324 (2020).
- [40] W. Kob and H. C. Andersen, Testing mode-coupling theory for a supercooled binary Lennard-Jones mixture: The van Hove correlation function, *Phys. Rev. E* **51**, 4626 (1995).
- [41] T. A. Weber and F. H. Stillinger, Local order and structural transitions in amorphous metal-metalloid alloys, *Phys. Rev. B* **31**, 1954 (1985).
- [42] S. J. Plimpton, Fast parallel algorithms for short-range molecular dynamics, *J. Comp. Phys.* **117**, 1 (1995).
- [43] M. P. Allen and D. J. Tildesley, *Computer Simulation of Liquids* (Clarendon, Oxford, 1987).
- [44] J. C. Qiao, Q. Wang, J. M. Pelletier, H. Kato, R. Casalini, D. Crespo, E. Pineda, Y. Yao, and Y. Yang, Structural heterogeneities and mechanical behavior of amorphous alloys, *Prog. Mater. Sci.* **104**, 250 (2019).
- [45] K. Kosiba, D. Söpu, S. Scudino, L. Zhang, J. Bednarcik, and S. Pauly, Modulating heterogeneity and plasticity in bulk metallic glasses: Role of interfaces on shear banding, *Int. J. Plast.* **119**, 156 (2019).
- [46] M. L. Falk and J. S. Langer, Dynamics of viscoplastic deformation in amorphous solids, *Phys. Rev. E* **57**, 7192 (1998).

- [47] G. P. Shrivastav, P. Chaudhuri, and J. Horbach, Heterogeneous dynamics during yielding of glasses: Effect of aging, *J. Rheol.* **60**, 835 (2016).
- [48] A. Ghosh, Z. Budrikis, V. Chikkadi, A. L. Sellerio, S. Zapperi, and P. Schall, Direct observation of percolation in the yielding transition of colloidal glasses, *Phys. Rev. Lett.* **118**, 148001 (2017).
- [49] R. Jana and L. Pastewka, Correlations of non-affine displacements in metallic glasses through the yield transition, *J. Phys.: Mater.* **2**, 045006 (2019).
- [50] N. V. Priezjev, The effect of thermal history on the atomic structure and mechanical properties of amorphous alloys, *Comput. Mater. Sci.* **174**, 109477 (2020).
- [51] N. V. Priezjev, Spatiotemporal analysis of nonaffine displacements in disordered solids sheared across the yielding point, *Metall. Mater. Trans. A* **51**, 3713 (2020).
- [52] M. Singh, M. Ozawa, and L. Berthier, Brittle yielding of amorphous solids at finite shear rates, *Phys. Rev. Mater.* **4**, 025603 (2020).
- [53] R. Shi, P. Xiao, R. Yang, and Y. Bai, Atomic-level structural identification for prediction of localized shear deformation in metallic glasses, *Int. J. Solids Struct.* **191**, 363 (2020).
- [54] N. V. Priezjev, Aging and rejuvenation during elastostatic loading of amorphous alloys: A molecular dynamics simulation study, *Comput. Mater. Sci.* **168**, 125 (2019).
- [55] N. V. Priezjev, Accelerated rejuvenation in metallic glasses subjected to elastostatic compression along alternating directions, *J. Non-Cryst. Solids* **556**, 120562 (2021).
- [56] W.-P. Wu, D. Sopy, X. Yuan, O. Adjaoud, K. K. Song, and J. Eckert, Atomistic understanding of creep and relaxation mechanisms of $\text{Cu}_{64}\text{Zr}_{36}$ metallic glass at different temperatures and stress levels, *J. Non-Cryst. Solids* **559**, 120676 (2021).
- [57] N. V. Priezjev, Atomistic modeling of heat treatment processes for tuning the mechanical properties of disordered solids, *J. Non-Cryst. Solids* **518**, 128 (2019).
- [58] N. V. Priezjev, The effect of cryogenic thermal cycling on aging, rejuvenation, and mechanical properties of metallic glasses, *J. Non-Cryst. Solids* **503**, 131 (2019).
- [59] Q.-L. Liu and N. V. Priezjev, The influence of complex thermal treatment on mechanical properties of amorphous materials, *Comput. Mater. Sci.* **161**, 93 (2019).
- [60] N. V. Priezjev, Potential energy states and mechanical properties of thermally cycled binary glasses, *J. Mater. Res.* **34**, 2664 (2019).
- [61] B. Shang, W. Wang, A. L. Greer, and P. Guan, Atomistic modelling of thermal-cycling reju-

vention in metallic glasses (2020). arXiv:2012.01105

Figures

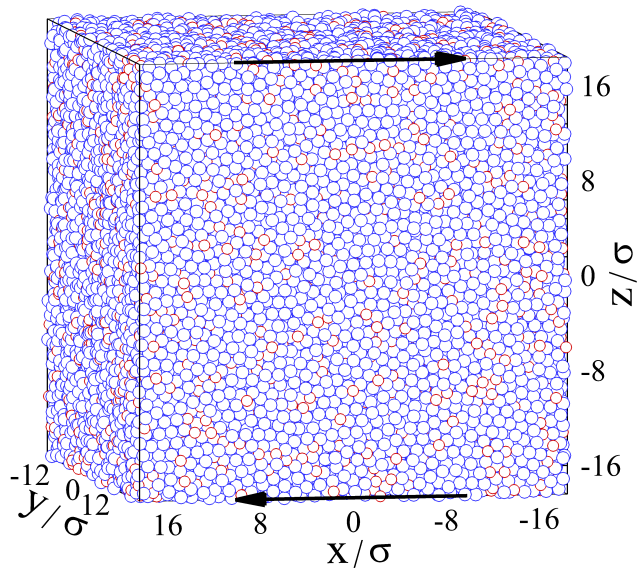


FIG. 1: (Color online) A snapshot of the *thermally annealed* glass at the temperature $T_{LJ} = 0.01 \varepsilon/k_B$. The system consists of 48 000 atoms of type *A* (large blue circles) and 12 000 atoms of type *B* (small red circles) in a periodic box of linear size $L = 36.84 \sigma$. Atoms are not shown to scale. The black arrows indicate the direction of oscillatory shear deformation along the xz plane.

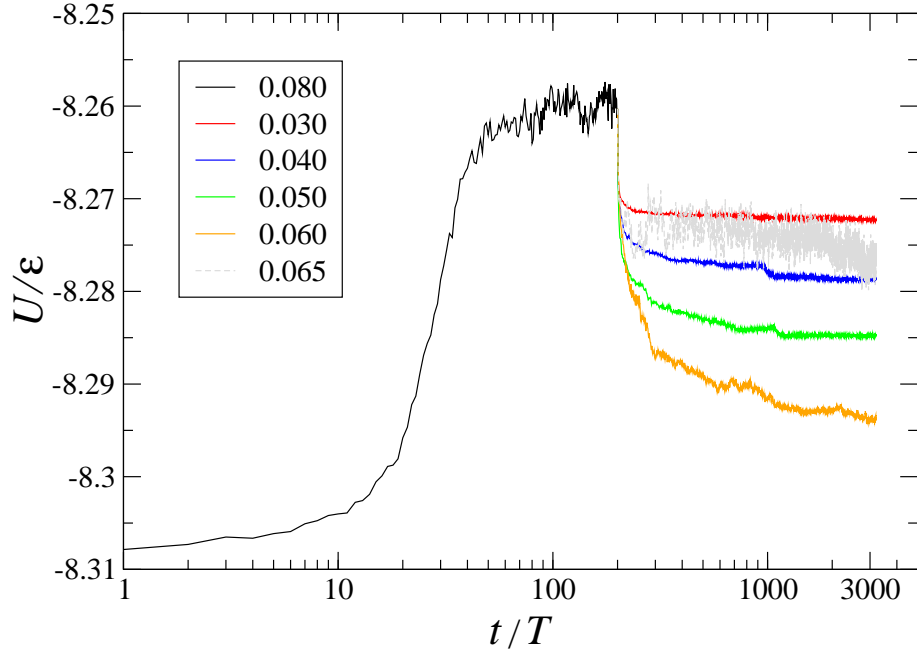


FIG. 2: (Color online) The dependence of the potential energy minima (at zero strain) on the number of cycles for the indicated values of the strain amplitude. The shear band was formed in the *thermally annealed* glass during the first 200 cycles at the strain amplitude $\gamma_0 = 0.080$ (the black curve). The system temperature is $T_{LJ} = 0.01 \varepsilon/k_B$ and the oscillation period is $T = 5000 \tau$.

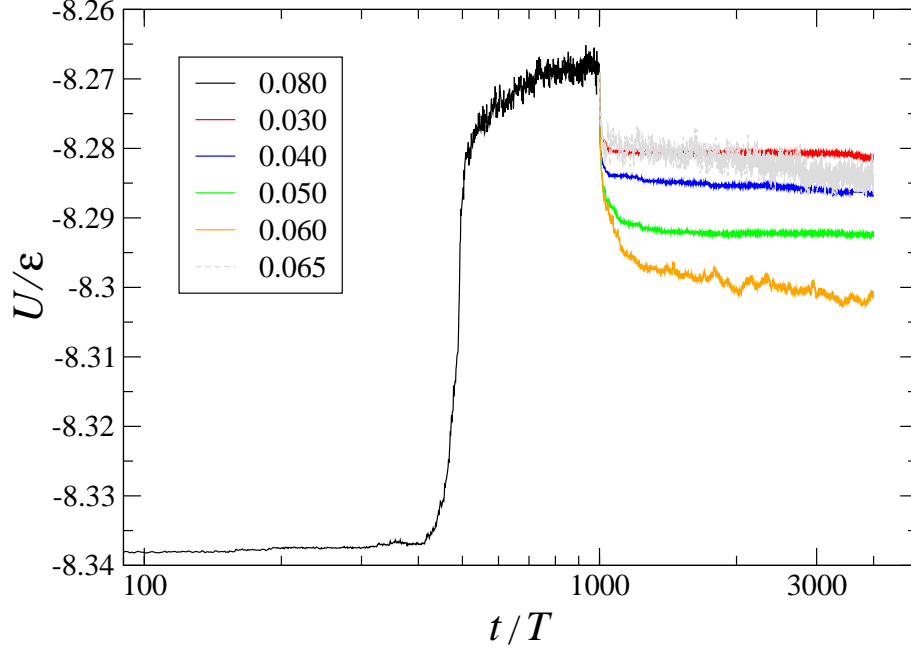


FIG. 3: (Color online) The variation of the potential energy (at the end of each cycle) as a function of the cycle number for the selected strain amplitudes. The shear band was introduced in the *mechanically annealed* glass after 1000 cycles at the strain amplitude $\gamma_0 = 0.080$ (the black curve; see text for details). The time is reported in terms of oscillation periods, *i.e.*, $T = 5000\tau$. The temperature is $T_{LJ} = 0.01 \varepsilon/k_B$.

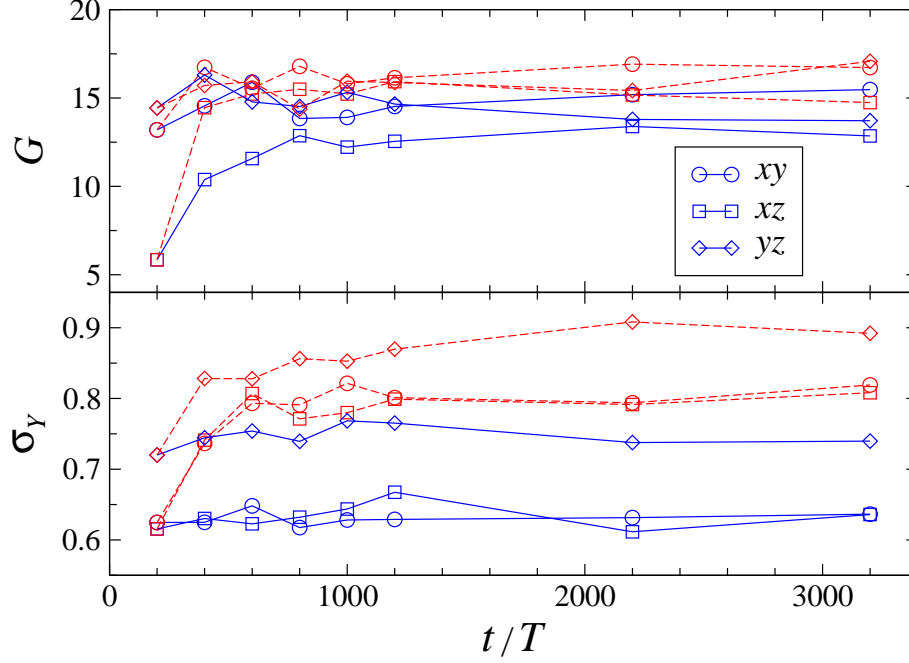


FIG. 4: (Color online) The shear modulus G (in units of $\varepsilon\sigma^{-3}$) and yielding peak σ_Y (in units of $\varepsilon\sigma^{-3}$) as a function of the cycle number for the *thermally annealed* glass. The startup continuous shear with the strain rate $\dot{\gamma} = 10^{-5} \tau^{-1}$ was applied along the xy plane (circles), xz plane (squares), and yz plane (diamonds). Before startup deformation, the samples were periodically deformed with the strain amplitudes $\gamma_0 = 0.030$ (solid blue) and $\gamma_0 = 0.060$ (dashed red). The time range is the same as in Fig. 2.

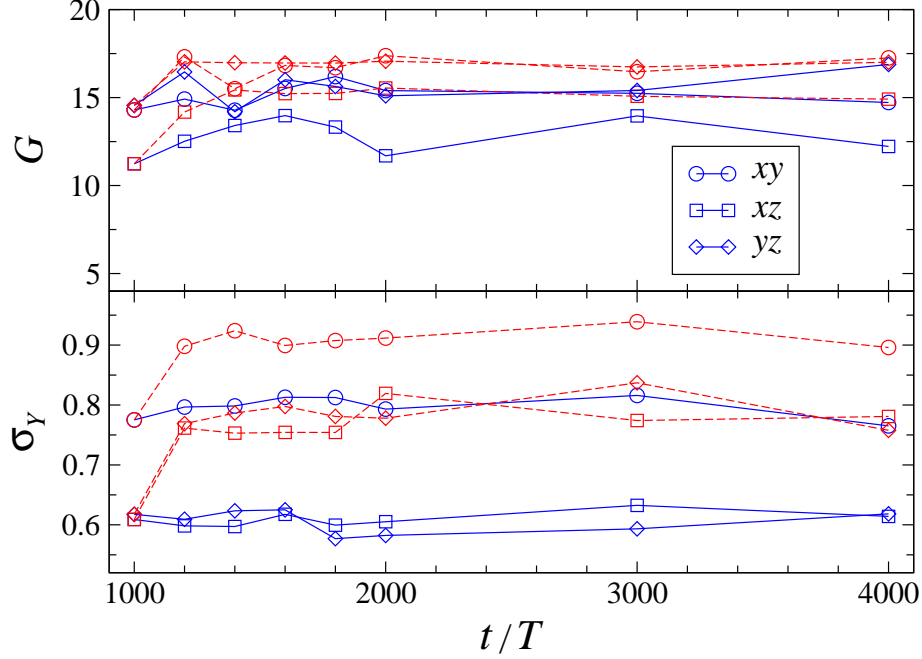


FIG. 5: (Color online) The shear modulus G (in units of $\varepsilon\sigma^{-3}$) and yielding peak σ_Y (in units of $\varepsilon\sigma^{-3}$) versus cycle number for the *mechanically annealed* glass. The startup shear deformation with the strain rate $\dot{\gamma} = 10^{-5} \tau^{-1}$ was imposed along the xy plane (circles), xz plane (squares), and yz plane (diamonds). Before continuous shear, the samples were cyclically deformed with the strain amplitudes $\gamma_0 = 0.030$ (solid blue) and $\gamma_0 = 0.060$ (dashed red). The same cycle range as in Fig. 3.

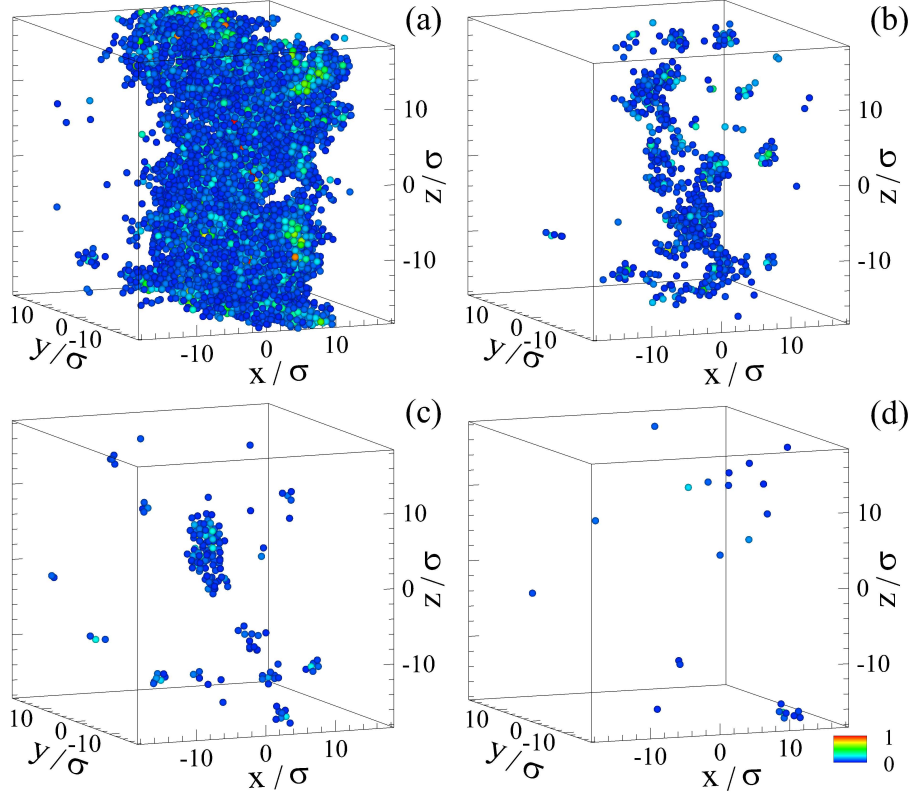


FIG. 6: (Color online) A series of snapshots of atomic configurations during periodic shear with the strain amplitude $\gamma_0 = 0.030$. The loading conditions are the same as in Fig. 2 (the red curve). The nonaffine measure in Eq. (3) is (a) $D^2(200T, T) > 0.04\sigma^2$, (b) $D^2(205T, T) > 0.04\sigma^2$, (c) $D^2(220T, T) > 0.04\sigma^2$, and (d) $D^2(300T, T) > 0.04\sigma^2$. The colorcode in the legend denotes the magnitude of D^2 . Atoms are not shown to scale.

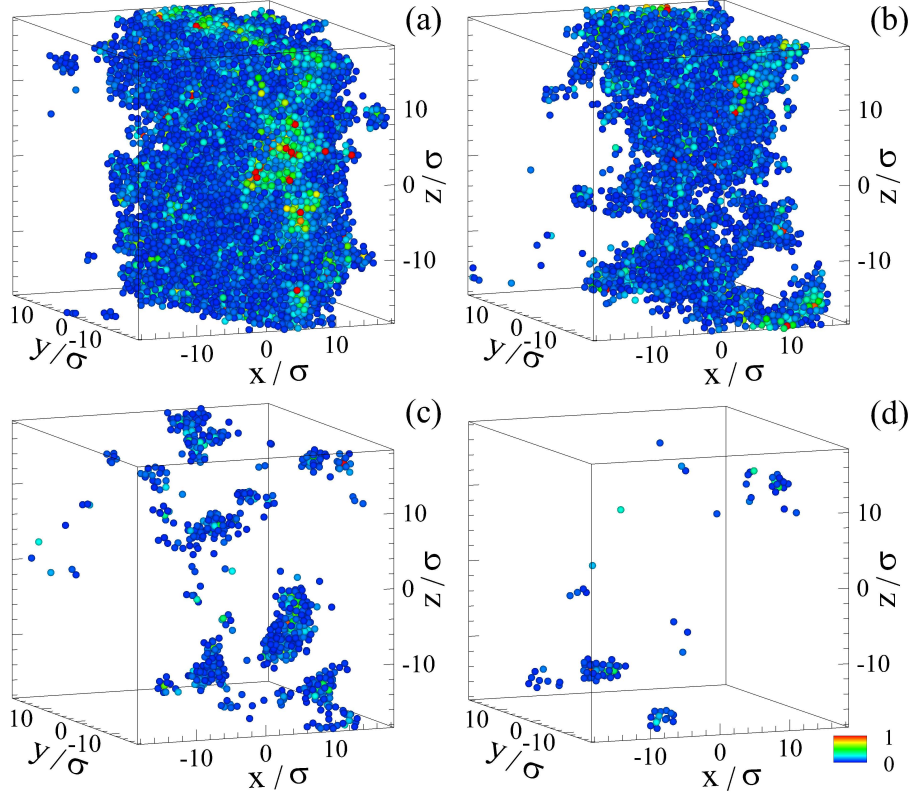


FIG. 7: (Color online) The position of atoms in the thermally annealed glass subjected to periodic shear with the strain amplitude $\gamma_0 = 0.060$. The corresponding potential energy is denoted by the orange curve in Fig. 2. The nonaffine measure is (a) $D^2(200T, T) > 0.04\sigma^2$, (b) $D^2(220T, T) > 0.04\sigma^2$, (c) $D^2(300T, T) > 0.04\sigma^2$, and (d) $D^2(1200T, T) > 0.04\sigma^2$. The magnitude of D^2 is defined in the legend.

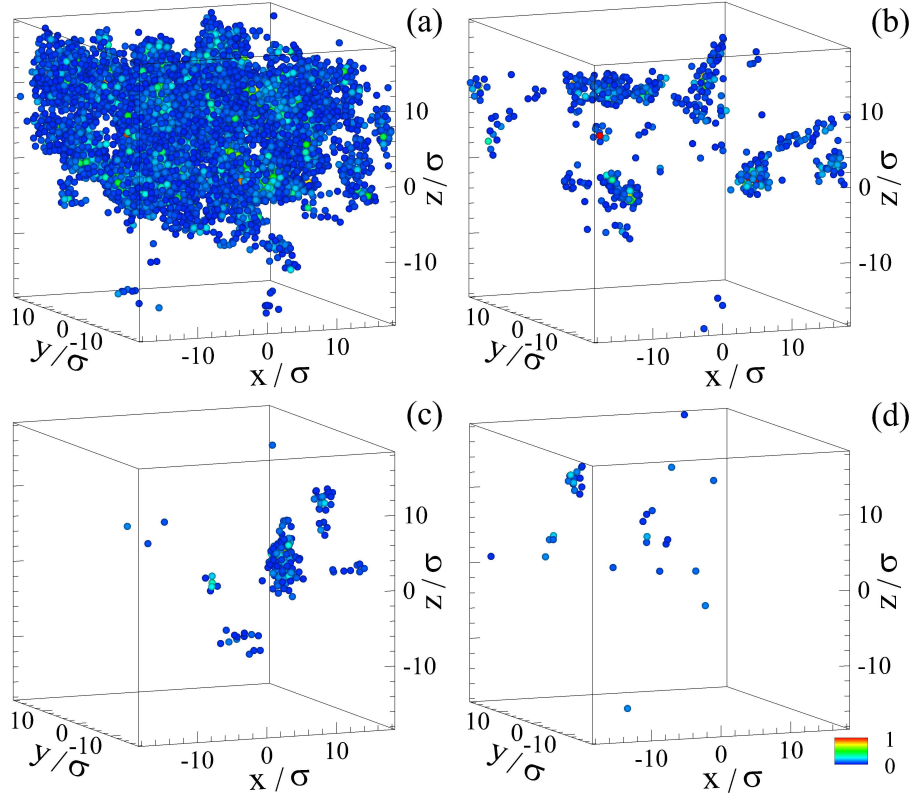


FIG. 8: (Color online) Instantaneous snapshots of the binary glass periodically sheared with the strain amplitude $\gamma_0 = 0.030$. The data correspond to the red curve in Fig. 3. The nonaffine quantity is (a) $D^2(1000T, T) > 0.04\sigma^2$, (b) $D^2(1005T, T) > 0.04\sigma^2$, (c) $D^2(1010T, T) > 0.04\sigma^2$, and (d) $D^2(1100T, T) > 0.04\sigma^2$. The colorcode denotes the magnitude of D^2 .

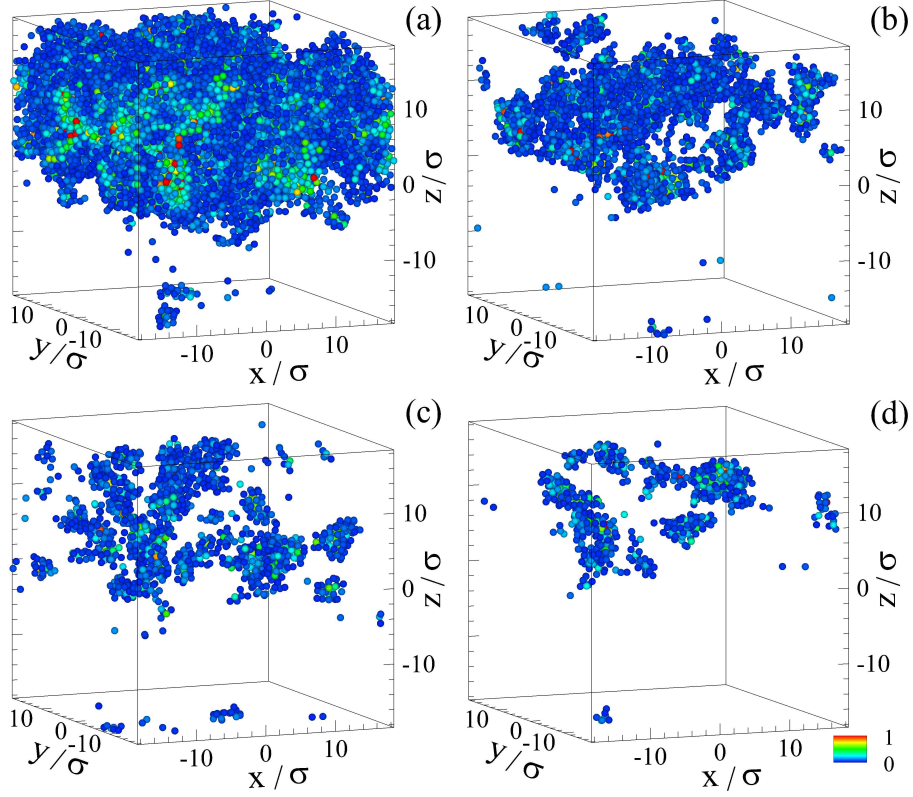


FIG. 9: (Color online) Atomic positions in the binary glass cyclically loaded at the strain amplitude $\gamma_0 = 0.060$. The data are taken from the selected time intervals along the orange curve in Fig. 3. The nonaffine quantity is (a) $D^2(1000T, T) > 0.04\sigma^2$, (b) $D^2(1100T, T) > 0.04\sigma^2$, (c) $D^2(1200T, T) > 0.04\sigma^2$, and (d) $D^2(3000T, T) > 0.04\sigma^2$. D^2 is defined in the legend.